9.5 Estimating Radar Beam Blockage from Thermal Noise with Verification by Precipitation Coverage

R.A. Rilling, J.C. Hubbert, and M. Dixon
National Center for Atmospheric Research, Boulder, CO USA, rilling@ucar.edu

28-December-2012

Introduction

The deployment of the NSF/NCAR S-PolKa radar to the Maldives as part of the DYNAMO experiment provided an opportunity to test various determinations of radar beam blockage under unique conditions. S-PolKa was deployed on the Addu Atoll, on a strip of land recovered from the ocean. The only blockage to the radar beam was due to a few nearby structures, but mostly by trees and vegetation along the ring of the atoll. Essentially, these trees formed a "stockade fence" of blockage on one side of the radar, with no possibility of blockage by terrain or any other features except the occasional ship. Blockage to the west was significant, with trees creating partial beam blockage to an elevation as high as 2.5 degrees; open ocean was mainly present to the east. (Since this note is concerned only with S-band beam blockage, the radar will be referenced as S-Pol, without the "Ka").

Fig. 1: Addu Atoll and the location of S-Pol

A full panoramic photo, taken from the S-Pol pedestal (3 m below the S-band dish center) is shown in Figure 2. In this figure, north is to each edge, and the vertical scale of the panorama has been exaggerated by a factor of four.

Three determinations of blockage are presented; note that all determinations are preliminary and somewhat incomplete, with work continuing:

- blockage determined from precipitation ratios compared at different elevation angles, and using different combinations of derived rainfall amounts (e.g., amounts estimated from reflectivity, only; amounts estimated from specific differential phase, or K_{DP})

- blockage determined from thermal noise along the radar beam

- an estimate of blockage from a simple model of obscuration of the beam by visible clutter

The second determination is of most interest, since a simple noise estimate can be made with just a few radar sweeps, while the determination based upon precipitation ratios requires integration over long periods when there is significant precipitation. A quick, simple determination might benefit deployments that are very short in duration, such as deployment of mobile radars, or deployment of S-Pol for short periods of time. Additionally, such a determination could be used by radars with only a single polarization. A noise estimate will also find blockage that is not characterized by analysis of digital elevation models (DEMs); for example, trees and buildings are not part of the DEM data set. It is not expected that the noise-power blockage estimate will be as robust as those based upon the extensive analysis of DEMs, or careful analysis of differential polarimetric variables (see Lang, et al., 2009 for a complete treatment); it is also unlikely that the noise blockage estimate will provide usable results when there are multiple instances of partial beam blockage along a single beam. The noise blockage estimate can, however, be an additional tool that may be usable on its own, or perhaps combined with other techniques for blockage estimation.

Noise Power Estimates from S-Pol

Atmospheric noise power as measured by S-Pol generally ranges from a high of -112 dBm to a low value of -114.5 dBm, depending mainly upon the elevation angle of the radar beam (lower power values at higher elevation angles). At high elevation angles, the radar beam intercepts less total atmosphere, atmosphere at lower path-integrated temperatures, and less total integrated water vapor, all of which results in lower beam noise power. Where the beam is blocked by clutter, the noise power is dependent upon the thermal microwave radiation emitted by the clutter. In cases of partial beam blockage, the measured noise power will be a combination of the clutter noise power and the atmospheric noise power for the current elevation angle.

For the DYNAMO project, S-Pol used a robust estimate of noise power determined by a new technique implemented by Dixon and Hubbert (2012). The estimate uses fuzzy logic incorporated in the Clutter Mitigation Decision algorithm (Hubbert, et al.. 2009), together with feature fields selected to be sensitive to a noise/no noise determination. Average noise for each beam was computed after algorithmic selection of noise gates for each beam. For the current study, the new noise estimates were used, but it was still required to select scans with very few meteorological echoes, in order to avoid having those echoes add to the passive noise power along a particular beam.

Blockage Estimates from Precipitation

A simple estimate of rainfall blockage was developed for S-Pol in DYNAMO, as part of an effort to correct total integrated, radar-estimated precipitation over the S-Pol domain. The rainfall blockage was determined only for the Z-R rainfall estimate. While polarization variable estimates of total rainfall were used in a relative way to normalize the Z-R estimates, these polar estimates were not essential to the Z-R blockage estimate, nor was blockage estimated specifically for any of the polar radar rainfall estimators.

For S-Pol, the MISMO Z-R rain rate estimate was used (Masaki Katsumata, personal communication with DYNAMO investigators):

RATE_ZH = zh_aa * (ZH ** zh_bb)

where
zh_aa = 0.027366
zh_bb = 0.69444
ZH in mm6/m3
RATE_ZH in mm/hr

An estimator based on K_{DP} was also referenced (from Sachidananda and Zrnic, 1987, eqn 9):

RATE_KDP = sign(K_{DP}) * kdp_aa * (|K_{DP}| ** kdp_bb).

where
kdp_aa = 40.6
kdp_bb = 0.866
RATE_KDP in mm/hr
specific differential phase (K_{DP}) in deg/km.

For 29 days of significant precipitation (as seen from S-Pol), the total estimated rainfall was time- and range-integrated along each azimuth/radial from S-Pol. The RATE_ZH values were only included if RATE_KDP existed (i.e., $K_{DP} > 0°$); due to the nature of the K_{DP} estimate, this removed occurrences of very light precipitation, or precipitation from small cumulus clouds (calculation of K_{DP} requires smoothing over at least 15 range gates, or a range of 2.25 km, and acts to filter-out small echoes and, coincidentally, echoes that are usually not well-developed in the vertical).

Figure 3 shows various estimates of azimuthally dependent time- and range-summed precipitation rates and ratios of those rates. Precipitation rates were summed in range (17 to 70 km) and time along each azimuth, after filtering on RATE_KDP exists. The RATE_KDP test ensured that sums were composed of the same population of rates, and indirectly ensures that rates are determined only from larger echoes, as noted, above. The range limit and the low elevation angles ensure that ice phase returns were not included in the estimates. Panel a) shows considerable variability in summed rates as azimuth changes; the RATE_KDP at 2.5° very closely tracks the RATE_ZH at the same elevation, except near 300 degrees, where the tallest blockage occurs. Panel b) provides ratios of the RATE_ZH sums to the RATE_KDP sum at the same elevation angle. Since RATE_KDP shows partial beam blockage (PPB) at 1.5° and even more complete blockage at 0.5°, neither of these tilts could be used to normalize RATE_ZH; RATE_KDP @2.5° was therefore used to first produce panel c), showing relative summed rates at each elevation, and then normalized to derive the fractional blockage shown in panel d). The fractional blockage as shown in panel d) is used as the comparison standard to evaluate blockage as estimated from radar noise power.

Optical Model of Beam Blockage

A simple model of optical blockage was created to compare with the precip- and noise-blockage estimates. The panoramic image was converted to a black-and-white mask (0 or 1), and logically “AND-ed” with a modeled beam image. This was done for each of the

Fig. 2: Panoramic image taken from the S-Pol pedestal, 3 m below the center of the dish; north is at each edge, and the vertical scale has been exaggerated by a factor of four to better show variations in the blockage.

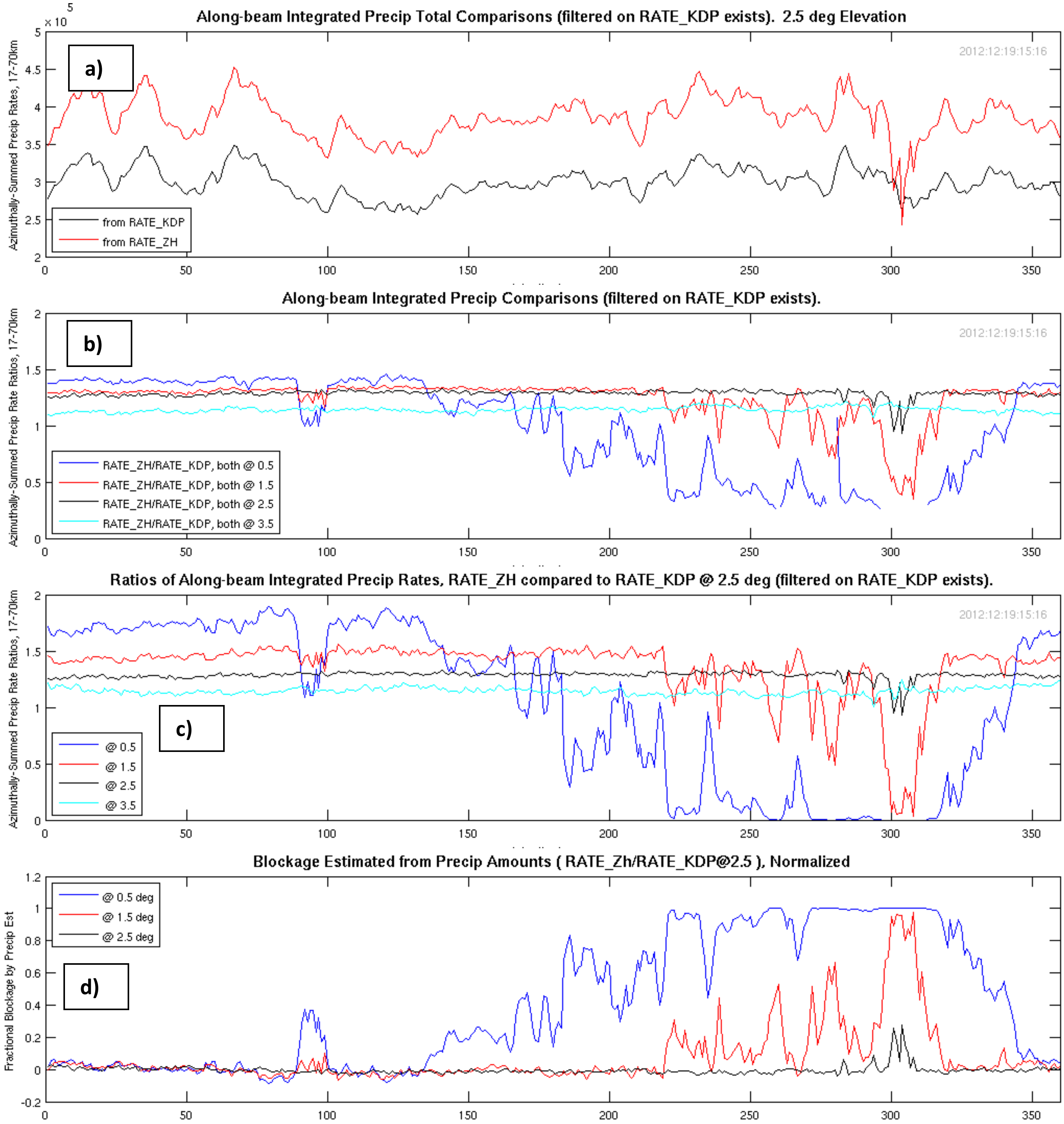

Fig. 3: Illustration of blockage determination from azimuthally dependent, range- and time-summed precipitation rates. a) RATE_ZH compared to RATE_KDP, filtered on RATE_KDP exists; the rates clearly show that RATE_KDP estimates are less impacted by partial beam blockage than RATE_ZH (see near 300 degrees); b) ratios of summed RATE_ZH to summed RATE_KDP at various elevation angles. c) ratio of summed RATE_ZH at various elevations, compared to the same summed RATE_KDP@2.5 degree elevation angle; d) the data from panel c, normalized by the average of the summed rate over the ocean, and subtracted from unity to provide a blockage fraction.

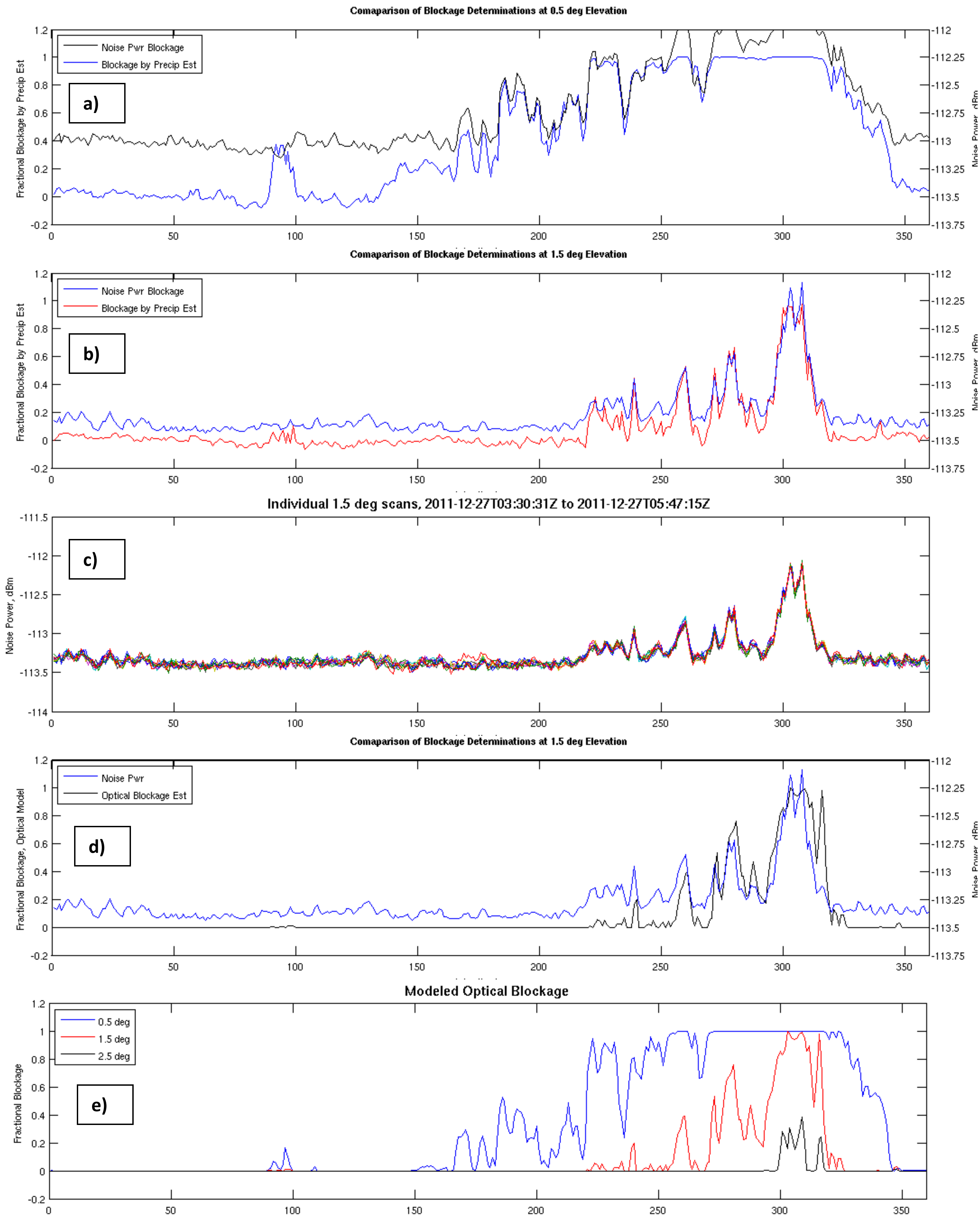

Figure 4: Various comparisons of radar beam blockage. a) shows multi-scan average radar noise power at 0.5° elevation angle, compared to blockage from estimated rain rate totals; b) is similar, for 1.5° elevation. Both a) and b)

indicate good tracking of the average noise power with estimated blockage. Panel c) shows the individual scan noise power for several sequential scans over a period of two hours; noise power is remarkably consistent. d) shows noise power compared to estimated optical beam blockage, both at 1.5° elevation. e) is modeled optical blockage for 3 elevations.

---

three lowest elevations scans. The S-Pol beam is very nearly circular and about 1° wide. However, since the beam is moving and uses off-index weighting to create indexed beams (i.e., beams at each whole azimuth angle), a 2° wide by 1° high elliptical model beam was used as a close approximation to the moving S-Pol beam. Modeled optical blockage is shown in Fig. 4, panels d) and e). Modeled optical blockage has many of the same characteristics as both the precipitation estimate of blockage and the noise power pattern. Differences are found over the wharf (near 90°) and for a single tree near 320° (the tree is actually quite sparse, and likely allows passage of most radar energy, but image filtering created a mostly opaque tree).

The optical model is likely to be of limited practical use in most radar siting situations, and is presented here only for completeness. Refinement of model assumptions and better procedure during panoramic image capture (the image was never intended for photogrammetric use) might improve the agreement of optical model to other blockage estimates.

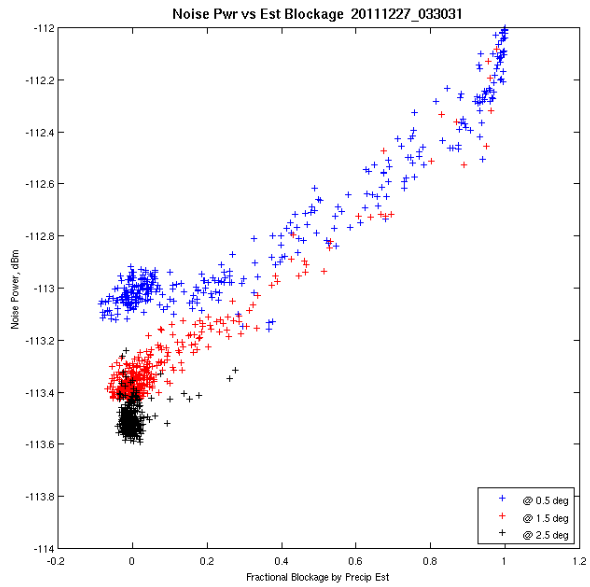

Figure 5: scatter plot of beam blockage vs measured noise power for several elevation tilts.

Comparison of Noise Power to Beam Blockage

Analysis of panels a) and b) in Fig. 4 shows that radar noise power very closely tracks the very fine details of a much more robust estimate of radar beam blockage. The analysis also shows that there are limitations to the use of noise power for blockage determination, particularly at the lowest elevation angles when the beam is only minimally blocked. This limitation is due to the lack of contrast between clutter microwave emission and atmospheric emission at low elevation angles. Fig. 5 shows a color-coded scatter plot for noise power vs blockage at three elevation angles. The cluster of points at which there is no beam blockage shows higher noise power with decreasing elevation angle, but more critically, the pattern of points "flattens out" at higher values of partial beam blockage as the elevation angle decreases.

Next Steps

S-Pol has a collection of data from past deployments at various sites throughout the world. The noise power technique will be evaluated for several of those past projects, particularly NAME, where Lang, et al.,(2009) have done extensive work in estimating PBB. Additional work will be focused on developing an equation for transformation of noise power directly into estimates of PPB. Consideration will be given to future special data collections, perhaps measuring noise power with the radar in non-transmit mode, and stepping the antenna in elevation by small fractions of a degree.

Conclusion

For the specific case of S-Pol in the Maldives, measured radar noise power is shown to have a very close relationship to a robust estimate of beam blockage. Extension of this technique is pending testing in other situations.

Acknowledgements

The National Center for Atmospheric Research is sponsored by the National Science Foundation. Any opinions, findings, conclusions, or recommendations are those of the authors, and do not necessarily reflect the views of the National Science Foundation.

References

Dixon, M. Hubbert, J.C., 2012: The separation of signal components in Doppler Radar returns. 7th European Conference on RADAR in Meteorology and Hydrology. SP-078

Hubbert, J. C., M. Dixon, S M Ellis, G Meymaris, 2009: Weather Radar Ground Clutter. Part I: Identification, Modeling, and Simulation. *J. Atmos. Oceanic Tech.*, **26**, 1165-80.

Lang, T. J., S. W. Nesbitt, L. D. Carey, 2009: On the Correction of Partial Beam Blockage in Polarimetric Radar Data. *J. Atmos. Oceanic Technol.*, **26**, 943–957.

Sachidananda M., D. S. Zrnic, 1987: Rain rate estimates from differential polarization measurements. *J. Atmos. and Oceanic Technol.*,**4**, 588-598.